J. Agromet 19 (1) : 21 – 38, 2005

# VARIABILITY OF NORMALIZED DIFFERENCE VEGETATION INDICES IN SUMATRA AND ITS RELATION TO CLIMATE ANOMALIES

## (Keragaman Indeks Vegetasi di Sumatera dan Hubungannya dengan Anomali Iklim)

**Erna Sri Adiningsih and Kustiyo**

Pusat Pengembangan Pemanfaatan dan Teknologi Penginderaan Jauh (Remote Sensing Research and Development Centre) - LAPAN

## ABSTRAK

Indeks vegetasi yang diperoleh dari data NOAA-AVHRR sudah umum digunakan sebagai indikator kehijauan dan kekeringan vegetasi. Kondisi iklim global dan regional diatas Sumatera mempengaruhi indeks vegetasi di Sumatera. Penelitian ini bertujuan mempelajari keragaman indeks vegetasi terutama di Sumatra dan hubungannya dengan El Nino - Southern Oscillation (ENSO) dan Indian Ocean Dipole Mode Event (DME). LAC NDVI periode 1996-2002 digunakan untuk menganalisa koefisien keragaman dan analisis korelasi kanonik. Keragaman NDVI yang tinggi ditemukan di pantai timur, bagian selatan dan bagian utara Sumatera, sedangkan di bagian barat dan tengah keragamannya rendah. Secara keseluruhan, keragaman NDVI selama monsun barat lebih tinggi daripada periode monsun timur. ENSO dan DME mempangaruhi indeks vegetasi di Sumatera pada lag 0,4,dan 5 bulan (nyata pada taraf 5%). Kontribusi terbesar diberikan oleh variable kanonik lag 1 ($R^2$=70.1%), sisa 29,9 % disebabkan oleh keragaman factor-faktor lainnya. Kerana korelasi dan signifikansi dari parameter iklim secara statistik tinggi, maka dapat digunakan sebagai prediktor NDVI di Sumatera. Diantara 6 *time lag* , parameter dengan lag 6 bulan mempunyai keragaman yang tertinggi. Namun, uji beda nyata menunjukkan bahwz korelasi kanonik pada lag 0,4,dan 5 yang mempunyai beda nyta tertinggi (pada taraf 95%). Struktur korelasi kanonik untuk parameter iklim pada lag 0 dan 1 didominasi oleh SOI dan anomaly SST. Sedangkan korelasi pada lag 2,5, dan 6 didominasi oleh SOI, anomaly SST, dan DMI. Berdasarkan hasil analisis tersebut, kami menyimpulkan bahwa analisis korelasi kanonik merupakan metode yang optimum untuk memprediksi NDVI di Sumatera pada lag 5 bulan menggunakan SOI, SSTA, dan DMI sebagai prediktor. Hasil ini menunjukkan bahwa parameter iklim dapat digunakan untuk memprediksi NDVI 5 bulan ke depan dengan baik di Sumatera.

**Kata kunci**: NDVI, Anomali suhu muka laut Nino 3,4. Dipole Mode Index, koefisien keragaman, dan korelasi kanonik.

## INTRODUCTION

Vegetation is one of fuel types which affect the vulnerability of land to fires. Vegetation greenness may reflect its moisture content, so that it might be considered as important factor of fire risks particularly in prone areas. Imagery from satellite has the ability to provide spatially comprehensive information for remote and inaccessible areas, making this valuable tool for research on regional scale analysis. Since the spectral variation of vegetation canopy is a function of photosynthetic activity and leaf area index, the use of visible and near infrared reflectance satellite data is possible for assessing the greenness and moisture content of vegetation. Several spectral vegetation indices have been developed over the last few decades from remotely sensed data. One of them that is commonly and widely used is Normalized Difference Vegetation Index (NDVI),

Penyerahan naskah : Januari 2005
Diterima untuk diterbitkan : April 2005

which is calculated from the difference between near infrared channel reflectance and red channel reflectance and normalized by their sum (Rouse *et al.*, 1973).

Time series of NOAA-AVHRR NDVI data are of importance for analysis of vegetation parameters on regional scale. NDVI derived from NOAA AVHRR data is thus essential to land fire risk research. Current findings on the use of NDVI as fire risk related parameter are the threshold of NDVI to determine fire risk in Kalimantan (Borneo) and the correlation between NDVI and leaf moisture in Jambi – Sumatra. Several papers also describe the capabilities of AVHRR-derived data for forest studies (Defries *et al.*, 1998; Kharuk *et al.*, 2003). A research on forest fire in Kalimantan has suggested that NDVI < 0.3 is the upper limit of area vulnerability to land fires (Hidayat, 1997). Other work found the correlation between NDVI and leaf moisture content over unburned area in Jambi - Sumatra is relatively high (Junaidi, 2002, unpublished). NDVI has also been widely used to monitor vegetation fires in Sumatra (Anderson *et al.*, 1999).

NDVI has proven to be a robust indicator of terrestrial vegetation productivity. Among climatic factors, precipitation and temperature strongly influence both temporal and spatial patterns of NDVI. On the other hand, climatic factors are also greatly influenced by global anomalies such as El Nino and Southern Oscillation. Previous studies have suggested prominent effects of such anomalies on climate over Indonesia (harger 1995a, 1995b; Puspito *et al.*, 2002). More over, western part of Indonesia, including Sumatra, is also considered to be affected by and Indian Ocean Oscillation (Saji *et al.*, 1999). Since NDVI has been suggested to be a reliable indicator of vegetation dryness, and thus risks to land fire, it has importance in any efforts attempting to develop land fire prevention activities particularly in Sumatra.

The objective of this research is to study the variability of vegetation indices of Sumatra and analyze the relation between ENSO, Dipole Mode Event and the predictability of vegetation indices of Sumatra. Hypothesis proposed in this research includes (1) NDVI variability varies between seasons and it is higher in the east coast and southern part of Sumatra than in the western and northern part of the island; and (2) vegetation indices in Sumatra are highly correlated with SST anomaly in Nino 3.4 area, SOI, and DMI, while the correlations vary between time lags.

## VEGETATION INDICES AND ITS VARIABILITY

Vegetation index is a satellite-derived parameter correlated with photosynthetic activities of vegetation and provides an indication of the greenness of vegetation (Sellers, 1985). Many formulas could be used to derive vegetation indices from remote sensing data. Diaz and Blackburn (2003) suggested ten formulas of vegetation indices. They are ratio vegetation index (RVI), normalized difference vegetation index (NDVI), perpendicular vegetation index (PVI), difference vegetation index (DVI), soil adjusted vegetation index (SAVI), transformed soil adjusted vegetation index (TSAVI), soil adjusted ratio vegetation index (SAVI2), first-order derivative green vegetation index derived using local baseline (IDL_DGVI), first-order derivative green vegetation index derived using zero baseline (IDZ_DGVI), second-order derivative green vegetation index derived using zero baseline (2DZ_DGVI). Diaz and Blackburn (2003) also found that based on the correlation coefficients for both LAI and percent canopy cover, the effects of background variations were most pronounced for NDVI, SAVI, and TSAVI, whereas SAVI2 and RVI were moderately affected.

Normalized Difference Vegetation Index (NDVI) is one of vegetation indices commonly used and also the most widely employed vegetation index and has proven to be useful in large scale vegetation monitoring. NDVI is broadly correlated in turn with several biophysical parameters such as the level of photosynthetic activity, transpiration rates (Sellers, 1985), the fraction of absorbed photosynthetically active radiation (FPAR), evapotranspiration (Running and Nemani, 1988), leaf area index (LAI), net primary production (NPP), (Tucker and Sellers, 1986; Prince, 1991; Diaz and Blackburn, 2003), and climate anomalies such as El Nino phenomenon (Verdin *et al*., 1999; Mennis, 2001).

Time series of NOAA-AVHRR NDVI data are important for the analysis of vegetation parameters on regional scale. Due to practical problems in collecting, pre-processing and archiving the data, full resolution LAC (Local Area Coverage) images are usually available only for short periods or for relatively small areas (Teillet *et al*., 2000). A more recent work used an approach to merge the temporally stable, high spatial resolution land cover variation derived from LAC images with the temporally variable NDVI information brought by GAC data. The approach provided good quality images in terms of both radiometric and geometric features (Maselli and Rembold, 2002).

Pan *et al*. (2003) has explored a new method of vegetation classification at large scales using multi-temporal 1-km NOAA AVHRR NDVI images. They found that NDVI could be used as parameter in vegetation classification system, thus indicated vegetation condition. Since vegetation condition is influenced by water availability, the inclusion of climate information, particularly rainfall, improved the classification from 63.3 % by using NDVI images alone to 71.4 %.

Kharuk *et al*. (2003) has used Global Vegetation Index (GVI) from NOAA-AVHRR to map forest landscapes in Siberia using a landscape-ecological approach. They used AVHRR data for classification of mountainous regions and the result showed that AVHRR derived maps were more detailed than existing landscape maps. AVHRR derived classification also compared favourably to larger scale forest management maps of softwood and hardwood forests.

NDVI has proven to be a robust indicator of terrestrial vegetation productivity. Among climatic factors, precipitation and temperature strongly influence both temporal and spatial patterns of NDVI. Wang *et al.* (2001) examined spatial responses of NDVI to precipitation and temperature during a 9-year period (1989-1997) in Kansas. Biweekly climate maps (precipitation and temperature) were constructed by interpolation of weather station measurements. Maps of biweekly growing season (March to October) NDVI were constructed for Kansas using NOAA-AVHRR NDVI images. Average precipitation is a strong predictor of the major east-west NDVI gradient. Deviation from average average precipitation explained most of the year-to-year variation in spatial patterns. NDVI and precipitation covaried in the same direction (both positive or negative) for 60-95% of the total land area. Minimum and average temperatures were positively correlated with NDVI, but temperature deviation from average was generally not correlated with NDVI deviation from average. Their results demonstrate that precipitation is a strong predictor of regional patterns of NDVI and, by inference, pattern of productivity.

Mennis (2001) explores the relationship between ENSO, captured by equatorial Pacific SST, and the interannual variation in vegetation vigour in the south-east USA, captured by AVHRR NDVI, for the period 1982-1992. The moving average and "baseline" methods (anomaly from the long term mean) were used to extract interannual patterns in the NDVI signature for croplands, deciduous forest and evergreen forests. The ENSO cycle was measured using mean SST anomalies and the percentage of SST cells above certain threshold values (e.g. 1.0 $^{o}$C above the long term

mean). The baseline method indicated a weak, yet persistent, negative correlation between ENSO warm phase events and vegetation vigour in the south-east USA. The moving average method yielded similar results but produced higher correlation values (-0.45 to -0.76, significant at the 0.01 level). Use of 2.0 $^{o}$C threshold SST anomaly was found to yield the highest correlation values as it captures not only the presence but also the intensity of ENSO warm phase events. These results indicate that there is a clear and recognizable, through inconsistent, relationship between ENSO and vegetation vigour in the southeast USA.

## EL NINO - SOUTHERN OSCILLATION (ENSO), INDIAN OCEAN DIPOLE MODE EVENT AND THEIR IMPACTS ON INDONESIA

The El Nino-Southern Oscillation (ENSO) is a coupled oceanic-atmospheric phenomenon consists of a sympathetic movement involving the Pacific Ocean and associated atmosphere in an essentially chaotic manner along the equator. The system oscillates between extremes of the so-called "warm events" usually lasting 1 or 2 year and involving movement of warm sea water from the western Pacific along the equator to impact on the west coast of the American continent and "cold event" associated with easterly trade-wind-induced flows of colder water from the eastern Pacific towards the west.

Historical data indicate that ENSO years as experienced by the Island of Java are either much warmer than non-ENSO years or only slightly, if it all, warmer than normal (non-ENSO) years. Using more than 40 year data, Harger (1995a) found that in recent years, since 1950, of the 9 ENSO warm events, the initial year tends to have been hot and dry for 6 (1951, 1957, 1963, 1972, 1982, 1991) and neutral or cool and wet for 3 (1968, 1976, 1986). The increasing annual trend in air-temperature exhibited by the mean monthly values over the period 1866-1993, for the Jakarta and the Semarang data taken together is 1.64 $^{o}$C (0.0132 $^{o}$C per year from 25.771 to 27.409 $^{o}$C). The 1.65 $^{o}$C difference between 1866 and 1991 can presumably be partitioned into: (1) urban heat-island effect, (2) effect of deforestation, (3) effect of secular micro-climate shift, (4) influence of general global warming with particular reference to the tropics.

In general ENSO years are associated with higher temperature than non-ENSO years, with a significant negative correlation between subsequent years which are thereafter systematically cooler. This may be because the ENSO event actively mixes excess heat energy into the ocean-sink to an extent that is in direct proportion to the outstanding positive temperature deviation. A weak ENSO, preceded by a relatively modest temperature build-up in the lead-up non-ENSO years, then results in limited mixing which leads to a relatively warm subsequent year while strong event leads to extensive mixing and so generally results in a following very much cooler year. Atmospheric temperature build-up possibly associated with the greenhouse effect may be coupled to an increasingly wider temperature swing in west and central Java associated with the warm pool influence but anchored by the ocean-sink (Harger, 1995a).

According to Harger (1995b), information drawn from meteorological records in the southeast Asia clearly indicates that each ENSO event is unique in terms of the signature which it imposes on the rainfall and temperature from location to location. Nevertheless, a strong underlying pattern within the context of each event, itself apparently initiated or molded by the character of the preceding years, can be detected. This pattern permits relatively circumscribed predictions of

forward conditions (drought intensity) for 2-3 year, to be made once the event "locks in" for the duration of the warm event and at least 1 year beyond. The character of the intervening non-ENSO years can also be projected but in a more tenuous, though fairly regular manner.

For the available historical data, all markedly upward-moving traces eventually delivered a hot dry season in east Indonesia. This sort of tendency within non-ENSO blocks can thus serve as a caution in the sense that a very hot ENSO event is likely in the offing. The correlation between the cumulative temperature deviation of the inter-ENSO blocks in relation to the temperature deviation of the first ENSO year is 0.43. In the region of southeast Asia represented by Indonesia and the Philippines, relatively secure predictions concerning likely upcoming drought can be made specific instances once an ENSO event "locks in" for successive years (2-4) until the warm event set terminates. In the case of Java and within succeeding inter-ENSO years, further prediction can be made with reference to successive years in terms of the character of preceding years. This system, in conjunction with predictions generated by models could form the basis of prediction of drought or rainfall within dry season from one year to the next.

The 1997-1998 El Nino, the strongest in recorded history, manifested itself with a number of unusual features associated with the Pacific wind system. According to Chen *et al*. (2001) these features include: (1) an annual cycle of an east-west migration of a weakened wind speed zone between 2 $^{o}$N – 9 $^{o}$N; (2) an asymmetric see-saw process of trade wind variation between the two hemispheres in terms of relative intensity and central position; and (3) an 18-month cycle of meridional oscillations of the Pacific doldrums and trade wind belts. In addition, the commonly-used argument of trade wind relaxation in association with El Nino appears to be partly introduced, at least for the present case, by the 'tilt effect' of the Pacific zonal winds. These novel findings, revealed by the newly available multi-year TOPEX altimeter data, may help to improve existing theories on El Nino formation, and may also contribute to its future prediction.

In the region of southeast Asia represented by Indonesia and the Philippines, relative secure predictions concerning likely upcoming droughts can be made in specific instances once an ENSO event "locks in" for successive years (2-4) until the warm event terminates. In the case of Java and within succeeding inter-ENSO years, further predictions can be made with reference to successive years in terms of the character of preceding years (Harger, 1995).

Saji *et al.* (1999) found other prominent oscillation of the atmosphere over Indian Ocean. The oscillation is characterized by posotive sea surface temperature anomaly at western part of Indian Ocean and negative sea surface temperature (SST) anomaly at eastern part of the Ocean (west of Sumatra). The oscillation is called Dipole Mode Event (DME). Various impacts of DME were indentified as flood in Kenya, east coast of Africa, and India, and contraryly droughts in Indonesia, east China, and Korea.

Dipole Mode Event is developed in subtropics of south Indian Ocean during summer. The initiation includes surface wind changes over Sumatra to southeastward which will increase local upwelling, raise thermocline, and decrease sea surface temperature. Coller waters in east Indian Ocean will induce easterlies along the equator, increase cooling of equatorial east Indian Ocean, and increase warming in west Indian Ocean. Warming in west part of the ocean will cause Ekman region over 10$^{o}$ S and it will spread westward (Webster *et al*., 1999).

During normal summer monsoon, Indian Ocean climate system is characterized by cooler SST in the western part and warmer SST in the eastern part, and symetric SST distribution in the

equatorial eastern part, OTCZ (Oceanic Tropical Convergenze Zone) is situated in the south of equator and causes rainfall of about 10 mm/day in the area, surface wind over southeast Indian Ocean weakens. During DME, changes will take place: cooling of SST in southeast Indian Ocean, asymetric SST distribution over equator, easterlies and passat over southeast Indian Ocean strengthen and spread out across equator, OTCS dissapears and convection over west Indian Ocean strengthen since SST is warmer than normal. This configuration is commonly called positive Dipole Mode. In fact, a negative Dipole Mode is also developed following/preceding positive DME with a converse configuration (Rao et al., 2001, 2002).

An index has been suggested to indentify DME, called Dipole Mode Index (DMI). Intensity of DME is represented by gradient of SST anomaly between western part of equatorial Indian Ocean (50°- 70°E and 10°S-10°N) and southeastern part of equatorial Indian Ocean (90°-110°E dan 10°S-0°) (Saji *et al*., 1999).

DME greatly depends on wind strenght over southern part of Indonesia during southeast monsoon. If southeast monsoon strengthens, DME may occur. DME in 1972, 1994, and 1997 coincided with the onset of El Nino during east monsoon (May-September) and it caused severe droughts in Indonesia (Mihardja *et al*., 2002). However, mechanism of the oscillation development is still not understood well. Several hypothesis suggested that this mode was related to ENSO (Alan *et al*., 2001), but other scientists suggested that this mode was an independent air-sea interaction over Indian Ocean and not affected by ENSO (Saji, 2000). Meanwhile, Webster *et al*. (1999) and Murtugudde *et al.* (2000) found a weak interaction between Indian Ocean and Pacific Ocean oscillations. Mihardja *et al.* (2002) found an interaction between ENSO, DME, and monsoon related to Indonesian region. According to Li *et al*. (2002), DME differs from ENSO because of several reasons: differences in relationship of cloud phase-SST between warm and cold pools, inversion of zonal wind basic position, slope of east-west thermocline, effects of Asia monsoon and its negative feedback on DME.

Furthermore, Saji *et al.* (1999) using 40 year observation data also indentified six DMEs, that is in 1961, 1967, 1972, 1982, 1994, and 1997. Rao *et al*. (2002) suggested that during the last 127 years, there were 14 positive strong DMEs and 19 negative strong DMEs, but only 5 positive DMEs and 7 negative DMEs coincided with ENSO. In other words, about 65 percent of DME does not coincide with ENSO.

Several studies have identified statistically significant correlations between Pacific sea surface temperature anomalies and NDVI anomalies in Southern Africa. Cross validation techniques suggested a more useful relationship for regions of wet anomaly than for regions of dry anomaly. Observed 1998 NDVI anomaly patterns were consistent with this result. Wet anomalies were observed as expected, but wide areas of expected dry anomalies exhibited average or above-average greenness. Cross-validation statistics suggest that Nino3 SSTs are more accurate predictors of increased greenness in the north Africa than decreased greenness in the south Africa (Verdin *et al*., 1999). Their results reveal that cross-validation has been shown to be a powerful measure of the expected performance of equatorial Pacific SST for forecasting Southern Africa NDVI.

Mennis (2001) has also indentified statistically significant correlations between Pacific sea surface temperature anomalies and NDVI anomalies in Southern Africa. Cross validation techniques suggested a more useful relationship for regions of wet anomaly than for regions of dry anomaly. Observed 1998 NDVI anomaly patterns were consistent with this result. Wet anomalies were observed as expected, but wide areas of expected dry anomalies exhibited average or above-average

greeness. Cross-validation statistics suggest that Nino3 SSTs are more accurate predictors of increased greenness in the north Africa than ddecreased greenness in the south Africa. Their results reveal that cross-validation has been shown to be a powerful measure of the expected performance of equatorial Pacific SST for forecasting Southern Africa NDVI.

## DATA AND METHODS

### AVHRR and Climatic Data

Daily LAC NOAA-AVHRR data of February 1996 to December 2002 were collected from LAPAN (Indonesian Institute of Aeronautics and Space) Ground Station in Jakarta. The data consists of NOAA-12 and NOAA-14. Global climatic data of the same period were also collected from NCEP-NOOA website. The climatic data consists of sea surface temperature anomaly (SSTA) over Nino 3.4 region (covers area between 5N - 5S and 170 W - 120 W) and Southern Oscillation Index (SOI) which indicates the difference between Tahiti air pressure and Darwin air pressure at mean sea level.

### AVHRR Data Processing

AVHRR data were pre-processed to obtain radiometrically and geometrically corrected data of Sumatra. Band 1 and 2 of the data were then processed to derive LAC NDVI using equation as follows:

**NDVI = (C2 - C1) / (C1+C2)**

C1 is albedo of channel 1 (red) AVHRR and C2 is albedo of channel 2 (near infrared) AVHRR respectively. The albedo of each channel is determined by digital number, gain and intercepts values of the channel. Gain and intercept values were obtained from the header of the data after radiometric correction were accomplished. Maximum composite of daily LAC NDVI for one month were used to obtain monthly NDVI images for LAC datasets from February 1996 to December 2002. NDVI values of 22 areas represent all provinces in Sumatra were then extracted to make time series of NDVI for each location.

### Data Analysis

Variability of NDVI for each area in Sumatra was analyzed based on coefficient of variance (CV). The greater the CV the greater the variability of NDVI. CV is calculated using equation as follows:

CV = (SD / MEAN) * 100

With SD is standard deviation and MEAN is arithmatic average of NDVI parameter.

Canonical Correlation Analysis (CCA) is multivariate statistical technique to analyze the correlation among two variable sets. Using this technique of analysis, a complex relation structure of two variable sets could be described. The objective of the analysis is to find linear combination of p independent variables which have maximum correlation with q linear combination of dependent variables. General equation of CCA is:

$$Y_1B_1 + Y_2B_2 + Y_3B_3 + ...Y_nB_n = A_0 + X_1A_1 + X_2A_2 + X_3A_3 + ...X_nA_n$$

Canonical correlation analyses (CCA) includes several steps in computing several parameters of CCA. Firstly, canonical correlation coefficients are obtained by establishing a correlation matrix (R). The structure of matrix is as follows:

$$\mathbf{R} = \begin{bmatrix} \mathbf{R}_{XX} & \mathbf{R}_{XY} \\ \mathbf{R}_{YX} & \mathbf{R}_{YY} \end{bmatrix}$$

where: $R_{XX}$ = correlation matrix for X variable set, $R_{YY}$ = correlation matrix of Y variable set, $R_{XY}$ $R_{YX}$ = correlation matrix between X and Y.
Each element of the matrix was coumputed by:

$$r_{XY} = \frac{n\sum XY - \sum X \sum Y}{\left[\sqrt{n\sum X^2 - (\sum X)^2}\right]\left[\sqrt{n\sum Y^2 - (\sum Y)^2}\right]}$$

Eigenvalue ($\lambda$) was then computed based on R matrix using the following equation:

$$\left|\mathbf{R}_{XX}^{-1}\mathbf{R}_{XY}\mathbf{R}_{YY}^{-1}\mathbf{R}_{YX} - \lambda^2\mathbf{I}\right| = 0$$

Eigenvalue was used to obtain eigenvector, which comprised of canonical variable coefficients. Eigenvector was calculated using equations:

$$\left(\mathbf{R}_{XX}^{-1}\mathbf{R}_{XY}\mathbf{R}_{YY}^{-1}\mathbf{R}_{YX} - \lambda^2\mathbf{I}\right)\mathbf{a} = 0$$

$$\left(\mathbf{R}_{YY}^{-1}\mathbf{R}_{YX}\mathbf{R}_{XX}^{-1}\mathbf{R}_{XY} - \lambda^2\mathbf{I}\right)\mathbf{b} = 0$$

The eigenvectors are a and b, which are canonical coefficients or canonical weights.
Canonical variables can be constructed using eigenvector consist of [p, q] sets as follow:

$$\begin{array}{ll} \mathbf{V_1} = a_1\underline{\mathbf{X}} & \mathbf{W_1} = b_1\underline{\mathbf{Y}} \\ \mathbf{V_2} = a_2\underline{\mathbf{X}} & \mathbf{W_2} = b_2\underline{\mathbf{Y}} \\ \cdot \quad \cdot & \\ \cdot \quad \cdot & \\ \mathbf{V_p} = a_p\underline{\mathbf{X}} & \mathbf{W_q} = b_q\underline{\mathbf{Y}} \end{array} \qquad \textbf{where:} \quad \underline{X} = \begin{bmatrix} X_1 \\ \vdots \\ X_p \end{bmatrix} \quad \underline{Y} = \begin{bmatrix} Y_1 \\ \vdots \\ Y_q \end{bmatrix}$$

Canonical correlation coefficients were the computed by employing :

$$r_{V,W} = \frac{\mathrm{Cov}(V,W)}{\sqrt{\mathrm{Var}(V)\mathrm{Var}(W)}} = \frac{\mathbf{a}'\mathbf{R}_{XY}\mathbf{b}}{\sqrt{(\mathbf{a}'\mathbf{R}_{XX}\mathbf{a})(\mathbf{b}'\mathbf{R}_{YY}\mathbf{b})}}$$

Data variance explained by each variable set can be obtained as follows:

$$DataVariance = \frac{\lambda_i}{\sum \lambda_i}$$

Further analyses on canonical variable sets is based on the limit of cumulative variance, which is 80 percent (Dillon and Goldstein, 1984).
Hypothesis test is accomplished as follows:

$H_o$ : $\rho_i = 0$, there is no sgnificant correlation between $i^{th}$ canonical variable sets.
$H_1$ : $\rho_i \neq 0$, there is no sgnificant correlation between $i^{th}$ canonical variable sets.

The last steps in CCA are determination of dominant variables and interpretation of canonical variables. Two techniques can be used:

a. Canonical Weight: indicates the contribution on the variability of canonical variables.
b. Canonical Loading: measures simple correlation between original variables and canonical variables. It reflects variance and contribution on canonical variables. The larger the loading the more important the loading in canonical variable derivation.

## RESULT AND DISCUSSION

### Variability of NDVI

Vegetation index variability in Sumatra for the period of 1996 to 2002 was analyzed based on its variance coefficients (CV). The results were then plotted spatially as shown in Figure 1 and 2. Figure 1 shows spatial NDVI variability in Sumatra for west monsoon (September to February) and Figure 2 shows variability for east monsoon (March to August).

From Figure 1 and 2 we see that variability of NDVI varies between seasons. The NDVI variability in Sumatra is summarized in Table 1. As depicted from Figure 1 and 2 it showed that during west monsoon (represented by September to February) the variability of NDVI on November was the highest and it is the lowest on January. Meanwhile during east monsoon (represented by March to August) the variability of NDVI on June was the highest and it the lowest on March. It was also shown that NDVI variability varied spatially. High variability was found on the eastern coast part, south part, and northern part of the island. The western and central parts of the island had low variability.

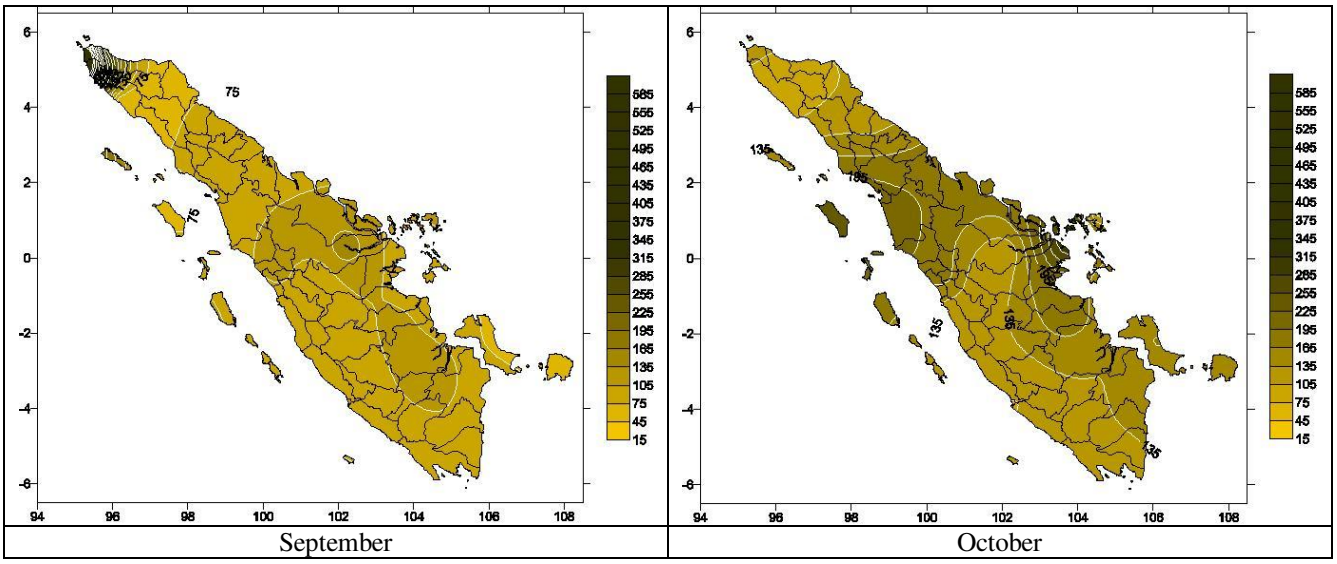

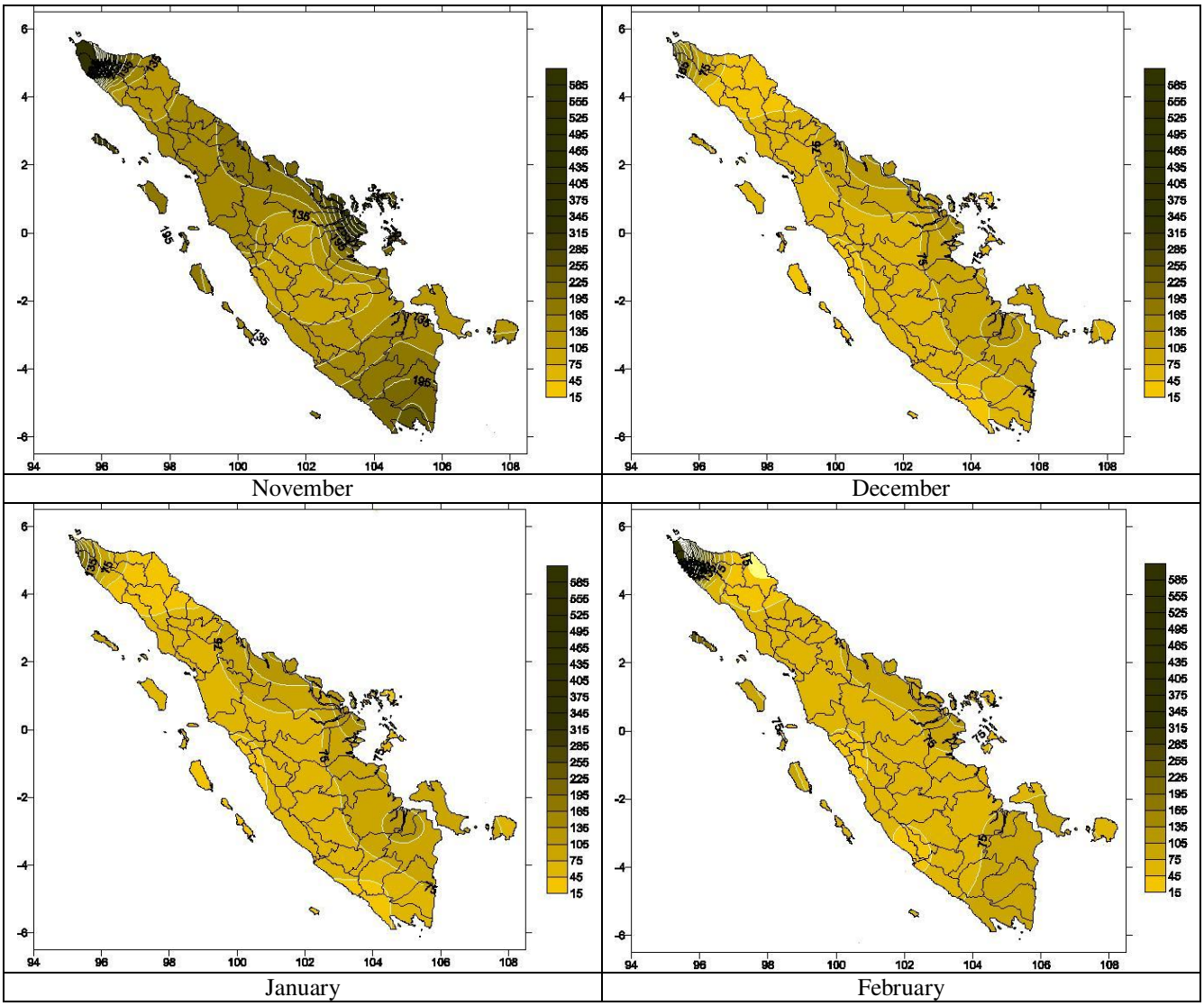


Figure 1. Distribution of monthly NDVI variability in Sumatra as indicated by average coefficient of variance for west monsoon (September to February).

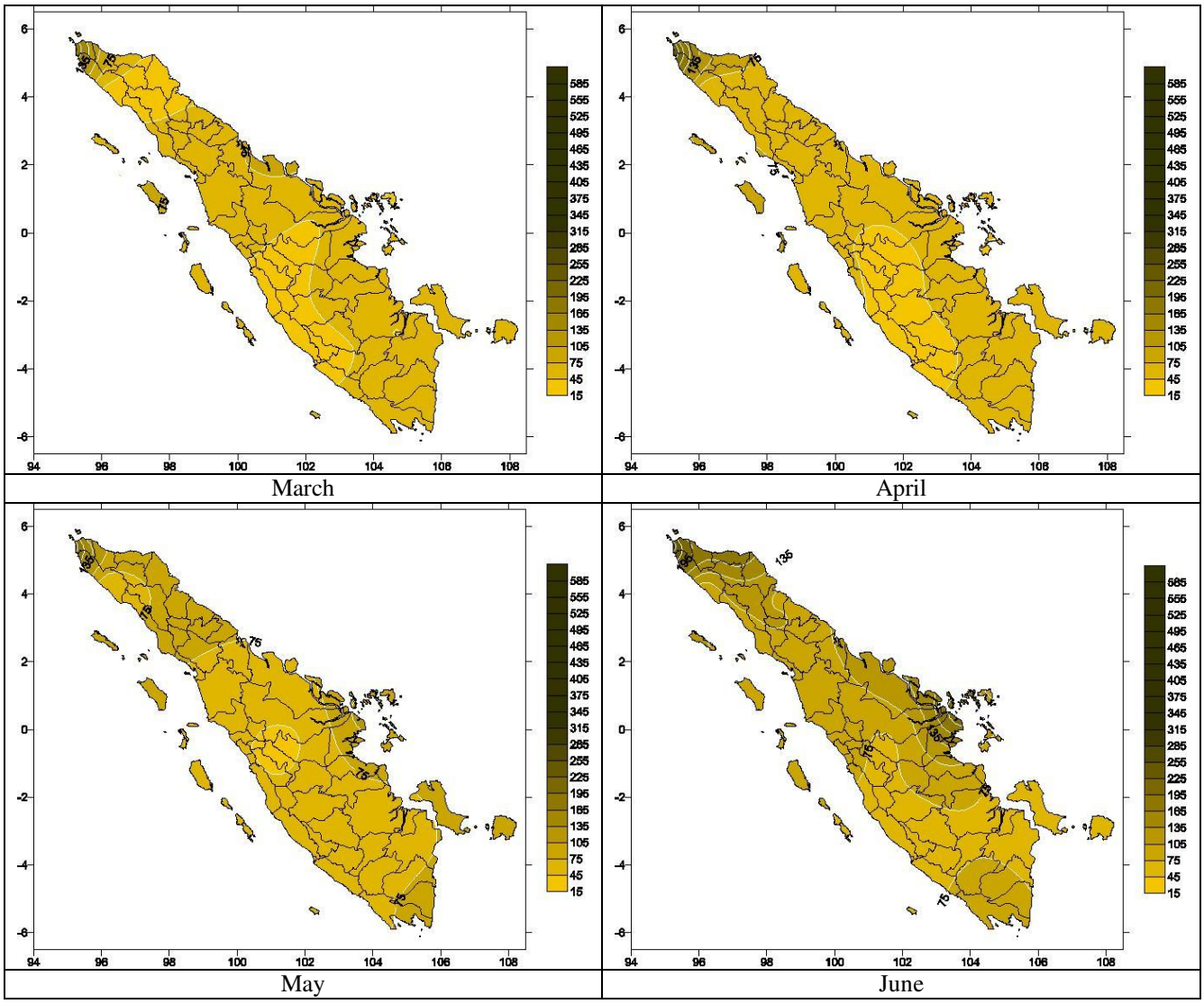
March
April
May
June

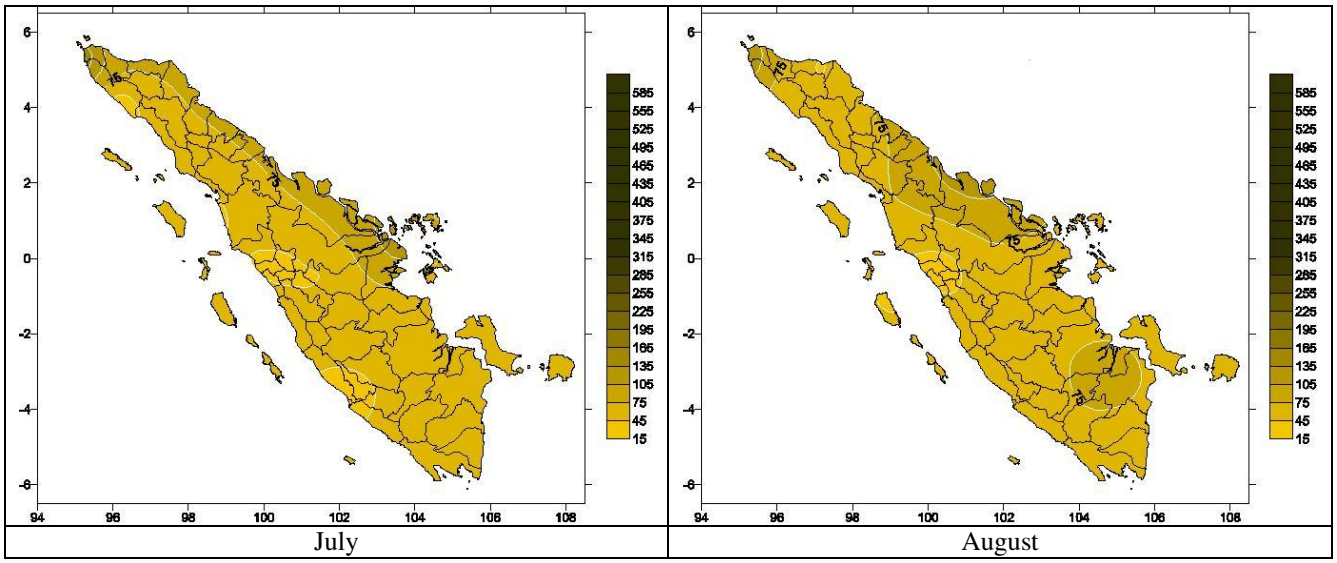


Figure 2. Distribution of monthly NDVI variability in Sumatra as indicated by average coefficients of variance for east monsoon (March to August).

As a whole, NDVI variability in Sumatra during west monsoon was higher than during east monsoon. Minimum CV was 15.17 and reached on August, while maximum CV was 1468.88 and reached on November. Since only southern part of Sumatra is affected by monsoon, this part of the island has NDVI which varies more than the most northern part (except in northmost part). It means that any anomaly in monsoon circulation will greatly affect NDVI in southern Sumatra rather than northern part.

Table 1. Summary of monthly coefficients of variance for NDVI in Sumatra

| CV | JAN | FEB | MAR | APR | MAY | JUN | JUL | AGS | SEP | OCT | NOV | DEC |
|---|---|---|---|---|---|---|---|---|---|---|---|---|
| Mean | 75.20 | 112.25 | 63.41 | 72.34 | 80.23 | 110.43 | 70.47 | 69.40 | 132.26 | 151.90 | 238.65 | 198.28 |
| Min | 22.65 | 28.99 | 33.31 | 29.00 | 37.47 | 54.03 | 33.99 | 15.17 | 46.83 | 75.56 | 86.99 | 64.63 |
| Max | 316.25 | 1104.98 | 216.40 | 294.74 | 235.26 | 297.51 | 181.95 | 145.24 | 976.89 | 368.11 | 1468.88 | 745.52 |

Canonical Correlation of ENSO (El Nino - Southern Oscillation) and DME (Dipole Mode Event) with Vegetation Index (NDVI) in Sumatera

Based on 21 NDVI variables in Sumatra and 3 climate variables (SOI, SSTA, and DMI), three canonical variable sets, V1 and W1, V2 and W2, V3 and W3, were established. Canonical correlations for the three variable sets are presented in Table 2.

Table 2. Canonical Corrrelation Coeficients

| Canonical Variable Sets | Canonical corrrelation coeficients for each time lag | | | | | | |
|---|---|---|---|---|---|---|---|
| | Lag 0 | Lag 1 | Lag 2 | Lag 3 | Lag 4 | Lag 5 | Lag 6 |
| 1 | 0.838 | 0.763 | 0.750 | 0.749 | 0.796 | 0.796 | 0.794 |
| 2 | 0.776 | 0.697 | 0.712 | 0.645 | 0.728 | 0.740 | 0.666 |
| 3 | 0.631 | 0.617 | 0.523 | 0.625 | 0.583 | 0.692 | 0.586 |

From Table 2 we can see that V and W canonical variables were highly correlated. Canonical correlations for the three variable sets of 0 to 6 month time lags are more than 50 percent and the highest correlation was 83.8 percent. Table 2 also shows that to an extent the longer the time lag the lower the correlation. This results indicate that climate parameters (SOI, SSTA, and DMI) not only highly affect NDVI in Sumatra but also significantly as shown by P-value (Table 3). It is important to note from Table 3 that ENSO and DME affect vegetation indices in Sumatra significantly for time lags of 0, 4, and 5 month (significant level at 5 %), while for the remaining time lags the significance is less. For prediction purposes, however, it can be said that the optimum time lag was 5 months meaning that climate parameters is able to be used to predict NDVI for 5 months ahead.

Table 3. Significance Test of Canonical Correlations

| Time Lag | lag 0 | lag 1 | lag 2 | lag 3 | lag 4 | lag 5 | lag 6 |
|---|---|---|---|---|---|---|---|
| P-Value | **0.00** | 0.10 | 0.22 | 0.22 | **0.04** | **0.01** | 0.11 |

Significance is indicated by P-value computed using Wilks' Lambda
Bold numbers indicates high significance.

**Relation between climate parameters and vegetation indices**

Contribution of independent variable sets on the variability of dependent variable sets was also analyzed to assess the relationship between climate parameters and vegetation indices. Based on computation, squared canonical correlation coefficients were then obtained. The results for the three variable sets are presented in Table 4.

Table 4. Squared Canonical Corrrelation Coefficients

| Canonical Variable Sets | Squared Canonical Corrrelation Coeficients for each Time Lag | | | | | | |
|---|---|---|---|---|---|---|---|
| | Lag 0 | Lag 1 | Lag 2 | Lag 3 | Lag 4 | Lag 5 | Lag 6 |
| 1 | 0.701 | 0.582 | 0.563 | 0.560 | 0.633 | 0.633 | 0.630 |
| 2 | 0.603 | 0.486 | 0.507 | 0.417 | 0.530 | 0.547 | 0.444 |
| 3 | 0.398 | 0.381 | 0.274 | 0.390 | 0.340 | 0.479 | 0.343 |

Table 4 shows relatively great contribution of climate variable sets in affecting NDVI variable sets. The greatest contribution was given by the 1st canonical variable of lag 1 ($R^2$=0.701). This means that 70.1 percent of NDVI variability can be explained by DMI, SOI, and SSTA parameters. Meanwhile, about 29.9 percent of NDVI variability is caused by other factors. Since the correlation and significance of climate parameters was statistically proven to be high, they could be used as predictors of NDVI in Sumatra. This result is also similar to those which were suggested by previous works in attempting to predict NDVI using climate parameters (Verdin *et al*., 1999; Mennis, 2001). Unlike previous studies, except ENSO parameters this study also included Indian Ocean Oscillation or Dipole Mode Event (DME) parameter in the analyses. The result reveals that both ENSO and DME phenomena are highly and significantly correlated with NDVI in Sumatra.

Table 5. Data Variance Explained by each Canonical Variable Sets

| Canonical Variable Sets | | Explained Data Variance | Cumulative Data Variance |
|---|---|---|---|
| Lag 0 | 1 | 0.5187 | 0.5187 |
| | 2 | 0.335 | 0.8538 |
| | 3 | 0.1462 | 1 |
| Lag 1 | 1 | 0.4717 | 0.4717 |
| | 2 | 0.3202 | 0.792 |
| | 3 | 0.208 | 1 |
| Lag 2 | 1 | 0.4785 | 0.4785 |
| | 2 | 0.3815 | 0.86 |
| | 3 | 0.14 | 1 |
| Lag 3 | 1 | 0.4847 | 0.4847 |
| | 2 | 0.2716 | 0.7563 |
| | 3 | 0.2437 | 1 |
| Lag 4 | 1 | 0.5119 | 0.5119 |
| | 2 | 0.335 | 0.8469 |
| | 3 | 0.1531 | 1 |
| Lag 5 | 1 | 0.448 | 0.448 |
| | 2 | 0.3138 | 0.7618 |
| | 3 | 0.2382 | 1 |
| Lag 6 | 1 | 0.5637 | 0.5637 |
| | 2 | 0.2637 | 0.8274 |
| | 3 | 0.1726 | 1 |

Variance of NDVI which could be explained by each canonical variable set is presented in Table 5. From the table we can see that data variance explained by 1st canonical variable set is 0.5187 for lag 0, meaning that 51.87 percent of NDVI data is described by 1st canonical variable set of lag 0. Similarly, data variances of lag 1 to 6 respectively were highest for respective 1st canonical variable sets. The variance of 2nd canonical variable set was lower than the 1st variable set and the 3rd canonical variable set had the lowest data variance. Among the six time lags, variable set of 6-month time lag had the highest variance. This result reveals that the 1st variable set of lag 6 was the

best, followed by lag 0, lag 4, lag 3, lag 2, lag 1 and lag 5 respectively. However, this does not imply that 1st variable set of 6-month time lag is the best predictor of NDVI. Further analyses based on significance test and canonical weight should be done to prove this. Significance test as shown in Table 3 indicates that the canonical correlations of lag 0, lag 4, and lag 5 were highly significant (at level 95%).

To describe canonical correlation, it also is important to analyze cumulative variance. The structur of canonical correlation can be analyze if the independent data variance is more than 80 percent. As we can see from Table 5, this condition was fulfilled by cumulative variance of the 1st and 2nd variable sets of lag 0 (92.48%), lag 2, and lag 6 respectively. Meanwhile, cumulative variance of lag 1, lag 3, and lag 5 was more than 80 percent for the three variable sets.

Further analyses on canonical weight and canonical loading was needed to determine the dominance of each predictor variable set. Table 6 has showed that standardized canonical weights was most significant for the 1st variable set of lag 0, followed by lag 5 and lag 4 respectively. The table also indicates that 2nd variable set of lag 5 was highly significant. Those means that lag 5 has the most significant variable sets. Analyses on climate parameters showed that SSTA gave the greatest contribution to the 1st climate variable sets of lag 0, lag 2, lag 3, and lag 6, while SOI gave the greatest contribution to lag 1 and DMI to lag 4 and lag 5 respectively (see Table 7). The greatest contribution to the 1st NDVI variable sets of lag 0 was given by Bengkulu, lag 1 by Gunung Sitoli, lag 2 by Jambi, Palembang and Rengat, lag 3 by Rengat, lag 4 by Palembang, lag 5 by southern part of South Sumatra, and lag 6 by west Riau. Based on canonical weights we suggest that SSTA is the greatest contributor to NDVI variability in Sumatra. On the other side, SOI significantly contributed to NDVI variability only at lag 2 and DMI at lag 4 and 5.

Table 6. Standardized Canonical Weights for each Time Lag

| Canonical Variable Sets | lag 0 | lag 1 | lag 2 | lag 3 | lag 4 | lag 5 | lag 6 |
|---|---|---|---|---|---|---|---|
| 1 | **0.00** | 0.10 | 0.22 | 0.22 | **0.04** | **0.01** | 0.11 |
| 2 | 0.06 | 0.30 | 0.48 | 0.47 | 0.26 | **0.05** | 0.52 |
| 3 | 0.41 | 0.48 | 0.87 | 0.44 | 0.65 | 0.15 | 0.64 |

Bold numbers indicates very high significance, the rest indicates moderate to low significance.

Analyses on canonical loadings (Table 7) suggested that the structure of canonical correlations for climate variable sets at lag 0 and lag 1 were dominated by SOI and SSTA. Meanwhile the correlations at lag 2, lag 5, and lag 6 were dominated by SOI, SSTA, and DMI. The correlations at lag 3 and lag 4 were dominated by DMI and SSTA. The structure of canonical correlations for NDVI variable set at lag 0 were dominated by South Aceh and east of West Sumatra. Nevertheless, no location dominated the structure of canonical correlation of NDVI at lag 1 to lag 6. These results imply that the three climate parameters were appropriate to predict NDVI at lag 2, lag 5, and lag 6. Considering analyses on correlation coefficient and significance test, we suggest that canonical correlation analyses is optimum method to predict NDVI at time lag of 5 months using SOI, SSTA, and DMI as predictors.

Table 7. Canonical Loadings for each Time Lag at Several Locations

| Parameters | Lag 0 | Lag 1 | Lag 2 | Lag 3 | Lag 4 | Lag 5 | Lag 6 |
|---|---|---|---|---|---|---|---|
| | V1 | V1 | V1 | V1 | V1 | V1 | V1 |
| DMI | 0.23 | 0.49 | **0.59** | **0.72** | **1.00** | **0.93** | **0.80** |
| SOI | **-0.94** | **-0.99** | **-0.69** | -0.42 | -0.36 | **-0.62** | **-0.64** |
| SSTA | **0.89** | **0.88** | **0.97** | **0.84** | **0.59** | **0.85** | **0.93** |
| Location | W1 | W1 | W1 | W1 | W1 | W1 | W1 |
| ACEH 2 | **0.504** | 0.357 | 0.352 | 0.308 | 0.296 | 0.432 | 0.444 |
| PADANG 1 | **0.520** | 0.430 | 0.406 | 0.295 | 0.272 | 0.444 | 0.475 |
| PADANG 2 | 0.417 | 0.296 | 0.299 | 0.223 | 0.233 | 0.284 | 0.252 |
| SICINCIN | 0.214 | 0.078 | 0.035 | 0.103 | 0.370 | 0.285 | 0.260 |
| BANGKA 2 | -0.036 | -0.171 | -0.225 | -0.371 | -0.102 | -0.158 | -0.156 |

Bold numbers indicate canonical loadings of more than 0.5.

## CONCLUSION

During west monsoon (represented by September to February) the variability of NDVI on November was the highest and it is the lowest on January. High variability was found on the eastern coast part, south part, and northern part of the island. The western and central parts of the island had low variability. As a whole, NDVI variability in Sumatra during west monsoon was higher than during east monsoon.

ENSO and DME affect vegetation indices in Sumatra significantly for time lags of 0, 4, and 5 month (significant level at 5 %), while for the remaining time lags the significance is less. For prediction purposes, however, it can be said that the optimum time lag was 5 months meaning that climate parameters is able to be used to predict NDVI for 5 months ahead.

The greatest contribution was given by the 1$^{st}$ canonical variable of lag 1 ($R^2$=0.701), meaning that 70.1 percent of NDVI variability can be explained by DMI, SOI, and SSTA parameters. Meanwhile, about 29.9 percent of NDVI variability is caused by other factors. Since the correlation and significance of climate parameters was statistically proven to be high, they could be used as predictors of NDVI in Sumatra.

Among the six time lags, variable set of 6-month time lag had the highest variance. This result reveals that the 1$^{st}$ variable set of lag 6 was the best, followed by lag 0, lag 4, lag 3, lag 2, lag 1 and lag 5 respectively. However, this does not imply that 1$^{st}$ variable set of 6-month time lag is the best predictor of NDVI. Further analyses based on significance test and canonical weight should be done to prove this. Significance test indicates that the canonical correlations of lag 0, lag 4, and lag 5 were highly significant (at level 95%). The structure of canonical correlations for climate variable sets at lag 0 and lag 1 were dominated by SOI and SSTA. Meanwhile the correlations at lag 2, lag 5, and lag 6 were dominated by SOI, SSTA, and DMI. The correlations at lag 3 and lag 4 were dominated by DMI and SSTA.

Considering analyses on correlation coefficient and significance test, we suggest that canonical correlation analyses is optimum method to predict NDVI in Sumatra at time lag of 5 months using SOI, SSTA, and DMI as predictors.

## ACKNOWLEDGEMENTS

This research was supported by funding from Riset Unggulan Terpadu (RUT) X under the Ministry of Research and Technology. Special thanks are due to Sudarman and Aendi Subyantoro for their work in NOAA-AVHRR raw data processing. The authors is also grateful to Dianis Santinira for her help in statistical data processing.

## REFERENCES

Alan, R *et al*. 2001. Is There An Indian Ocean Dipole, and Is It Independent of The El Nino Southern Oscillation?. CLIVAR Exchanges 21:1-4

Anderson, I.P., Irfan D. A, Muhnandar. 1999. Vegetation Fires In Sumatra, Indonesia : A Firest Look at Vegetation Indices and Soil Dryness Indices In Relation to Fire Occurrence. Balai Inventarisasi dan Perpetaan Hutan Wilayah II dan Kanwil Kehutanan dan Perkebunan. Palembang.

Chen, G., R. Ezraty, Y. He, and C. Fang. 2001. *Abnormal features of the Pacific wind system during the 1997-1998 El Nino*. Int. J. Remote Sensing, 22 (18): 3907-3912.

Defries, R.S., M. Hansen, J.G.R. Towshend, R. Sohlberg. 1998. *Global land cover classifications at 8 km spatial resolution: the use of training data derived from Landsat imagery in decision tree classifiers*. Int. J. Remote Sensing, 19: 3141-3168.

Diaz, B.M. and G.A. Blackburn. 2003. *Remote sensing of mangrove biophysical properties: evidence from a laboratory simulation of the possible effect of background variation on spectral vegetation indices*. Int. J. Remote Sensing, 24(1): 53-73

Harger, J.R.E. 1995a. *Air temperature variations and ENSO effects in Indonesia, the Philippines and El Salvador, ENSO patterns and changes from 1866-1993*. Atmospheric Environment, 29 (16): 1919-1942.

Harger, J.R.E. 1995b. *ENSO variations and drought occurrence in Indonesia and the Philippines*. Atmospheric Environment, 29 (16): 1943-1955.

Hidayat, A. 1997. *Membangun sistem pemantauan kekeringan vegetasi untuk peringatan dini kebakaran hutan menggunakan data penginderaan jauh*. Laporan Riset. Riset Unggulan terpadu III Bidang Teknologi Perlindungan Lingkungan (th.1995 –1997). Dewan Riset Nasional Kantor Menteri Negara Riset dan Teknologi, Jakarta.

Kharuk, V.I., K.J. Ranson, T.A. Burenia and E.V. Fedotova. 2003. *Mapping of Siberian forest landspaces along the Yenisey transect with AVHRR*. Int. J. Remote Sensing, 24 (1): 23-37.

Li, T, B. Wang, C.P. Chang, Y. Zhang. 2002. *A Theory for The Indian Ocean Dipole Mode*. International Pasific Research Center University of Hawaii. Honolulu.

Maselli, F. And F. Rembold. 2002. *Integration of LAC and GAC NDVI data to improve vegetation monitoring in semi-arid environments*. Int. J. Remote Sensing, 23(12): 2475-2488.

Mennis, J. 2001. *Exploring relationships between ENSO and vegetation vigour in the south-east USA using AVHRR data*. Int. J. remote Sensing, 22 (16): 3077-3092.

Mihardja *et al*. 2002. Interaksi Monsun-ENSO-DME di Perairan Indonesia. Pertemuan MIPA III. Bandung.

Murtugudde, R., J.P. McCreary, and A.C. Busalacchi. 2000. *Oceanic processes assosiated with anomalous events in the indian ocean with relevance to 1997-1998*. J. Geophys. Res., 105: 3295-3305

Pan, Y., X. Li, P. Gong, C. He, P. Shi and R. Pu. 2003. *An integrative classification of vegetation in China based on NOAA AVHRR and vegetation-climate indices of the Holdridge life zone*. Int. J. Remote Sensing, 24(5): 1009-1027.

Prince, S.D. 1991. *A model of regional primary production for use with coarse-resolution satellite data.* Int. J. Remote Sensing, 12:1313-1330.

Puspito, N.T., Z.L. Dupe, P.A. Winarso dan E.S. Adiningsih. 2002. *Prediksi El Nino/La Nina untuk Mitigasi Bencana Meteorologi pada Sistem Transportasi*. Kementerian Riset dan Teknologi.

Rao, S.A., S.K. Behera, Masumoto Y and T.Yamagata. 2001. *Interannual variability in the subsurface Indian Ocean with special emphasis on the Indian Ocean Dipole*. Deep Sea Research-II. Indian Ocean Dipole Homepage.

Rao, S.A., S.K. Behera, Y. Masumoto, T. Yamagata. 2002. Subsurface Interannual Variability Associated with The Indian Ocean Dipole. CLIVAR Exchanges 23:1-4.

Running, S.W. and R.R. Nemani. 1988. *Relating seasonal patterns of the AVHRR vegetation index to simulated photosynthesis and transpiration of forests in different climates*. Remote Sensing of Environment, 24: 347-367.

Saji, N.H. 2000. *The Ocean At Work During The Indian Ocean Dipole Mode*. Frontier newsletter.

Saji. N.H., B.N. Goswani, P.N. Vinayachandran, T. Yamagata. 1999. *A Dipole Mode In The Tropical Indian Ocean*. Nature 401: 360-363

Sellers, P.J. 1985. *Canopy reflectance, photosynthesis, and transpiration*. Int. J. Remote Sensing, 6: 1335-1372.

Teillet, P.M., N. El Saleous, M.C. Hansen, J.C. Eidenshink, C.O. Justice, and J.R.G. Townshend. 2000. *An evaluation of the 1-km AVHRR land dataset*. Int. J. Remote Sensing, 21: 1987-2021.

Tucker, C.J. and P. Sellers. 1986. *Satellite remote sensing of primary production*. Int. J. Remote Sensing, 7:1395-1416.

Verdin, J., C. Funk, R. Klaver, and D. Roberts. 1999. *Exploring the correlation between Southern Africa NDVI and Pacific sea surface temperatures: results for the 1998 maize growing season*. Int. J. Remote Sensing, 20(10): 2117-2124.

Wang, J., K.P. Price, and P.M. Rich. 2001. *Spatial patterns of NDVI response to precipitation and temperature in the central Great Plains*. Int. J. Remote Sensing, 22 (18): 3827-3844.